Original Research Article

Proposal and simulation of a Doubly Fed Induction Generator for the coastal zone of Benin

***Abstract*— In this paper, we propose the sizing of a Doubly Fed Induction Generator (DFIG) with a power of 690.747 kW for the coastal area of Benin. We start from the power density of the offshore wind potential of Benin obtained at 80 m at the sea surface to determine the power of the generator. Thanks to the geometrical, electrical and magnetic parameters obtained after sizing, we simulate the operation of the generator using the finite element analysis (FEA). This simulation is done by running the generator at nominal speed in supersynchronous mode. We obtain the curves of the powers and those of the flux densities in the air gap, as well as the various losses of the generator. We use the results of the electromagnetic model to develop the thermal model of the generator. The results of the thermal analysis obtained after simulation by the FEA allowed us to know the temperature values in each region of the DFIG.**

Keywords- DFIG; FEA; power density; electromagnetic model; thermal model

I. INTRODUCTION

The request for electrical energy in Benin is becoming more and more important every year and the coverage of the country in energy still remains a major problem today. Almost all of the electrical energy produced is distributed in urban areas, with an electrification rate of 67 % compared to only 18 % in rural areas. However, more than half of the population lives in rural areas. This represents an inequality. To propel the development of a country, electricity must be available for public lighting, households, schools and health centers. One of the measures of the Beninese government's action program is to develop renewable energies to improve the living conditions of the population by reducing their difficulties in accessing electrical energy[1], [2].

Several projects for the production of electrical energy from renewable sources are therefore underway. In this context, we propose here the sizing of a DFIG for the generation of electric energy by wind turbine. The goal that we aim is to produce a technical document exploitable by the manufacturers for the design of the DFIG adapted to the offshore wind profile of Benin.

The wind turbine power generation system (Figure 1) generally consists of a turbine that rotates using the kinetic energy of the wind. This turbine is usually coupled to a generator through a gearbox. The generator transforms the mechanical energy received by the turbine into electrical energy. The step-up transformer allows the connection to the distribution grid.

DFIG is the most commonly used generator in wind energy, especially in offshore environments, as it offers great operating advantages. This generator is connected on the stator side directly to the electrical grid while its rotor is connected to the grid via a converter. This latter includes an intermediate DC bus and two reversible AC-DC stages. The DFIG operates at a variable speed of about ±30% of the synchronous speed (Ω_s). It can operate in subsynchronous mode where the rotational speed (Ω) is lower than the synchronous speed ($\Omega < \Omega_s$) or in supersynchronous mode where the rotational speed is higher than the synchronous speed ($\Omega > \Omega_s$) [3]–[5] .

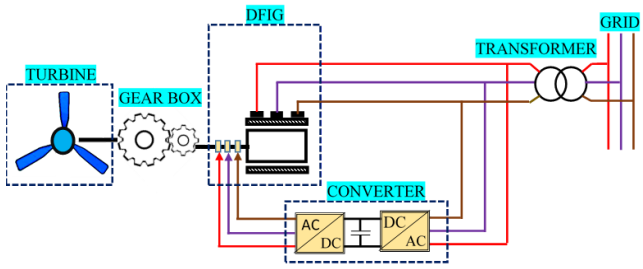

Figure 1. Wind turbine power generation system

This paper is subdivided into two main parts. In the first part we do the sizing and simulation of the DFIG for the chosen area. In the second part, we present the thermal model of the sized DFIG.

II. DFIG SIZING AND SIMULATION

To determine the power of the generator, we choose a zone located at sea at 10 km from the Beninese coast. The coordinates of this zone are 6.25°N in North latitude and 2.25°E in East longitude (figure 3).

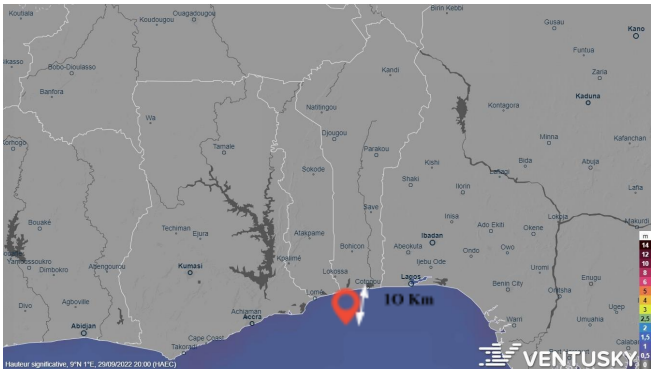

Figure 2. Coastal zone of Benin [6]

We choose a horizontal axis wind turbine located at a height of 80m from the sea surface. The curves of the distribution of the power density available at 80m in the exclusive economic zone of Benin are plotted and presented in [7].

We notice that the potential varies between $612\ W/m^2$ and $850.4\ W/m^2$. This is excellent for the production of offshore wind energy. By exploiting these curves, we deduce the power density (D_p) for the coordinates of the chosen area. Thus, we find that $D_p = 799.5336\ W/m^2$. The available wind power$\left(P_w\right)$ is given by the following equation (1) [8] :

$$P_w = D_p . \pi R^2 \quad (1)$$

Where P_w is the wind power, D_p the power density and R the radius of the turbine in m/s.

The aerodynamic power $\left(P_{ae}\right)$ recoverable by the turbine shaft is given by the relation (2).

$$P_{ae} = C_p . P_w \quad (2)$$

Where C_p is the power factor.

Assuming that all the aerodynamic power is transmitted to the generator then the power of the generator (P_{DFIG}) is equal to the recoverable aerodynamic power. Hence $P_{DFIG} = P_{ae}$.

For $C_p = 0.44$ and $R = 25m$ we obtain $P_{DFIG} = 690.747\ kW$.

The geometry of the DFIG that we want to size is shown in figure 4. We can see that it is composed of a wound slot stator and a wound slot rotor.

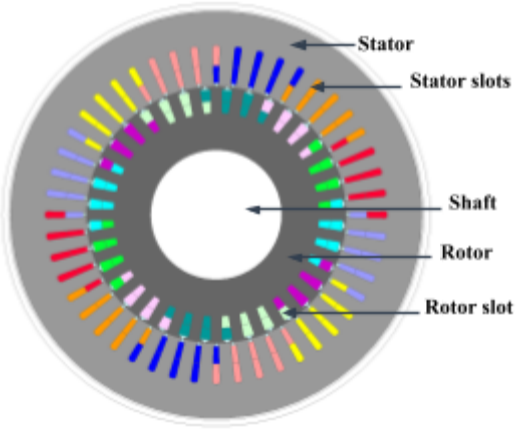

Figure 4 shows a cross-section of the DFIG indicating the geometrical parameters to be determined. The windings used in both the stator and the rotor are double layer.

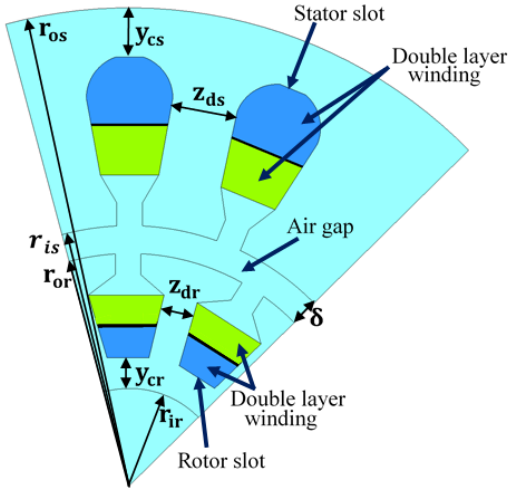

Figure 4. Cross-section of the DFIG

The first four geometrical parameters to be determined are: the inner radius of the stator $\left(r_{is}\right)$, the thickness of the air gap (ξ), the outer radius of the rotor $\left(r_{or}\right)$ and the length L of the generator.

The initial DFIG data are shown in Table 1.

TABLE I. INITIAL DFIG DATA

Designation	Symbol	Unite	Value
Power	P_G	kW	690.747
Stator Rated voltage	U_s	V	690
Rotor Rated voltage	U_r	V	690
Frequency	f	Hz	50
Number of pole pair	p	-	2
Rated slip	s	-	0.2
Efficiency	η	-	0.95
Power factor	cos $cos\ \varphi$	-	1
Air gap flux density	B_ξ	T	0.8

Synchronous speed	Ω_s	rpm	1500
Rated speed	Ω_n	rpm	1800
Number of stator slot	Q_s	-	48
Number of rotor slot	Q_r	-	36
Stack length/pole pitch	λ	-	1.3
form factor	k_f	-	1.1
Linear current density	A	kA/m	58.6
Flux density shape factor	α_i	-	0.64
Stator current density	J_s	(A/mm^2)	4.4
Rotor current density	J_r	(A/mm^2)	7
Stator chorded coil windings	ε_s		5/6
Rotor chorded coil windings	ε_r		7/9

The powers of the stator (P_s) and the rotor (P_r) of the generator have the formula [9], [10],[11]:

$$P_s = \frac{P_{DFIG}}{1+s} \quad (3)$$

$$P_r = |s|P_s \quad (4)$$

For the determination of r_{is} the following relation is used [12]:

$$r_{is} = \frac{1}{2}\left[\sqrt[3]{\frac{2.p^2 K_E P_s}{\eta\lambda f A.k_f \alpha_i \pi^3 B_\xi k_{bs} \cos\cos\varphi}}\right] \quad (5)$$

With:

$$K_E = 0.98 - .005p \quad (6)$$

And k_{bs} the stator winding factor defined by:

$$k_{bs} = \sin sin\left(\varepsilon_s . \frac{\pi}{2}\right) \times \frac{1}{2q_s \sin sin\left(\frac{\pi}{6q_s}\right)} \quad (7$$

With q_s the number of slots per pole and per phase of the stator such that:

$$q_s = \frac{Q_s}{6p} \quad (8)$$

In the same way the rotor winding factor k_{br} is defined by:

$$k_{br} = \sin sin\left(\varepsilon_r . \frac{\pi}{2}\right) \times \frac{1}{2q_r \sin sin\left(\frac{\pi}{6q_r}\right)} \quad (9$$

With q_r the number of slots per pole and per phase of the rotor such that:

$$q_r = \frac{Q_r}{6p} \quad (10)$$

The air gap thickness is determined by the following relationship (11):

$$\xi = \left(0.1 + .012\sqrt[3]{P_s}\right).10^{-3} \quad (11)$$

The outer radius of the rotor can be deduced from equations (5) and (11) by the relation:

$$r_{or} = r_{is} - \xi \quad (12)$$

The length of the generator is calculated by the formula:

$$L = \frac{\lambda\pi r_{is}}{p} \quad (13)$$

A. Stator dimension

At the stator we choose to use semi-closed rounded slots. The geometry and geometrical parameters associated with this slot are presented in figure 5.

We fix by experiment the opening of the slot hysm at $z_{s1} = 3\,mm$, the height of the slot hysm at $y_{s1} = 1\,mm$ and the height at the upper part of the slot hysm at $y_{s2} = 2.5\,mm$. We take $z_{s2} = 3.z_{s1}$ and $z_{s3} = 4.z_{s1}$. The section of the stator slot (A_{es}) is calculated by the following equation:

$$A_{es} = \frac{\pi D_{is} A}{k_{fi} Q_s J_s} \quad (14)$$

With D_{is} the inner diameter of the stator and k_{fi} the stator slot fill factor.

We establish the expression of y_{s4} as a function of A_{es} by equation (15).

$$y_{s4} = \frac{8A_{es} - z_{s1}^2(9\pi+12)}{28z_{s1}} \quad (15)$$

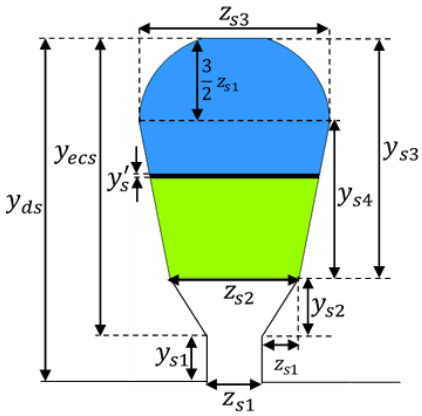

Figure 5. Stator slot geometry

The calculation of y_{s4} allows us to deduce the slot depth y_{s3}, the slot height y_{ecs} and the stator tooth height y_{ds} by the following system of equations:

$$\{y_{s3} = y_{s4} + \frac{3}{2}z_{s1}\, y_{ecs} = y_{s2} + y_{s3}\, y_{ds} = y_{ecs} + y_{1s}$$

The width of the tooth (z_{ds}) and the height of the stator yoke (y_{cs}) have the following expressions:

$$z_{ds} = \frac{\pi\left(D_{is} - 2y_{s1} + 2y_{s2}\right)}{Q_s} - 3z_{s1} \quad (17)$$

$$y_{cs} = \frac{\alpha_i \pi D_{is} B_\xi}{4pB_{ys}} \quad (18)$$

where B_{ys} is the flux density in the stator yoke equal here to 1.5T.

the external radius of the stator is therefore:

$$r_{os} = y_{cs} + r_{is} + y_{ds} \quad (19)$$

B. Rotor dimension

At the rotor we have chosen semi-closed slots of trapezoidal shape. On figure 6 we can see its different parameters.

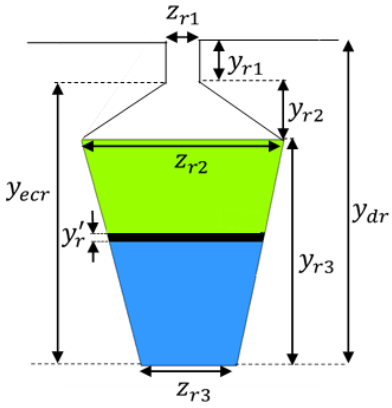

Figure 6. Stator slot geometry

The opening of the slot hysm, the height of the slot hysm and the height at the upper part of the rotor slot hysm are respectively: $z_{r1} = 2.5\,mm$, $y_{r1} = 1\,mm$ and $y_{r2} = 3\,mm$.

We first determine the cross-sectional area of the slot $\left(A_{er}\right)$ and the width of the rotor tooth $\left(z_{dr}\right)$ by the following relationships:

$$A_{er} = \frac{\pi D_{or} A}{k_{fi} Q_r J_r} \quad (20)$$

$$z_{dr} = \frac{\pi D_{or} B_\xi}{Q_r B_{tr}} \quad (21)$$

With D_{or} the external diameter of the rotor and B_{tr} the induction in the rotor teeth equal to 1.6T in our case.

Then, we determine the rotor slot depth y_{r3} by solving the following second-degree equation:

$$\frac{\pi}{Q_r} y_{r3}^2 + \left[z_{dr} - \frac{2\pi\left(r_{or} - y_{r1} - y_{r2}\right)}{Q_r}\right] y_{r3} + A_{er} = 0 \quad (22)$$

The height of the rotor slot $\left(y_{ecr}\right)$ and the height of the rotor tooth $\left(y_{dr}\right)$ are calculated by the following system:

$$\{y_{ecr} = y_{r2} + y_{r3}\, y_{dr} = y_{ecr} + y_{r1} \quad (23)$$

The height of the rotor y_{cr} is calculated by equation (24).

$$y_{cr} = \frac{\alpha_i \pi D_{or} B_\xi}{4pB_{yr}} \quad (24)$$

where B_{yr} is the flux density in the rotor yoke equal to 1.4T.

The expressions of the large base z_{r2} and the small base z_{r3} are presented in the system of equation (25).

.

$$\{z_{r2} = \frac{2\pi}{Q_r}\left(r_{or} - y_{r1} - y_{r2}\right) - z_{dr}\; z_{r3} = \frac{2\pi}{Q_r}\left(r_{or} - y_{r1} - y_{r2} - y_{r}\right.$$

The inner radius of the rotor has the formula:

$$r_{ir} = r_{or} - y_{dr} - y_{cr} \quad (26)$$

C. Determination of electrical parameters

We want the sized generator to be able to operate at a temperature of 115°C. The resistances of the stator $\left(R_s\right)$ and the rotor$\left(R_r\right)$ at this high temperature are calculated by the following equations [12] :

$$R_s = \frac{2\rho_{co_{115}^\circ} N_s \left(L + L_{end\_s}\right)}{A_{co\_s}} \quad (27)$$

$$R_r = \frac{2\rho_{co_{115}^\circ} N_r \left(L + L_{end\_r}\right)}{A_{co\_r}} \quad (28)$$

where $\rho_{co_{115}^\circ}$ is the copper resistivity at 115°, N_s and N_r are the number of turns per phase at the stator and rotor respectively, L_{end_s} and L_{end_r} are the end connection length at the stator and rotor respectively, A_{co_s} and A_{co_r} are the conductor cross section at the stator and rotor respectively.

A_{co_s} and A_{co_s} are defined by:

$$A_{co\_s} = \frac{I_{sn}}{a_1 J_s} \quad (29)$$

$$A_{co\_r} = \frac{I_{rn}}{a_1 J_r} \quad (30)$$

Where I_{sn} and I_{rn} are respectively the RMS currents at the stator and at the rotor defined by the equation system (31) and a_1 is the number of current paths in parallel equal here to 1.

$$\{I_{sn} = \frac{P_s}{\sqrt{3} U_s \eta \cos\cos\varphi}\; I_{rn} = s\frac{U_s}{U_r} I_{sn} \quad (31)$$

L_{end_s} and L_{end_r} are calculated by the relations (32) and (33) for a machine with 2 pairs of poles:

$$L_{end\_s} = 2y_1 - 0.02 \quad (32)$$

$$L_{end\_r} = 2y_2 - 0.02 \quad (33)$$

With y_1 and y_2 the coil span respectively at the stator and rotor defined by:

$$y_1 = \varepsilon_s \frac{\pi D_{is}}{2p} \quad (34)$$

$$y_2 = \varepsilon_r \frac{\pi D_{or}}{2p} \quad (35)$$

For the calculation of the stator and rotor leakage inductances, we use equations (36) and (37) [13].

$$L_s = \frac{12\mu_0 L N_s^2}{Q_s}\lambda_s \quad (36)$$

$$L_r = \frac{12\mu_0 L N_r^2}{Q_r}\lambda_r \quad (37)$$

With μ_0 the relative vacuum permeability, λ_s and λ_r the respective stator and rotor slots leakage geometrical permeance defined by the relations:

$$\lambda_s = k_{1s}\frac{y_{s4}-y_s'}{3z_{s2}} + k_{2s}\left(\frac{y_s'}{z_{s2}} + \frac{y_{s1}}{z_{s1}} + \frac{y_{s2}}{z_{s2}-z_{s1}}ln\left(\frac{z_{s2}}{z_{s1}}\right)\right) + \frac{y_s'}{4z_{s2}}$$

$$\lambda_r = k_{1r}\frac{y_{r3}-y_r'}{3z_{r2}} + k_{2r}\left(\frac{y_r'}{z_{r2}} + \frac{y_{r1}}{z_{r1}} + \frac{y_{r2}}{z_{r2}-z_{r1}}ln\left(\frac{z_{r2}}{z_{r1}}\right)\right) + \frac{y_r'}{4z_{r2}}$$

Where the constants k_{1s}, k_{2s}, k_{1r} and k_{2r} have the expression:

$$\{k_{1s} = 1 - \left(\frac{9}{16}\right)\varepsilon_1\ k_{2s} = 1 - \left(\frac{3}{4}\right)\varepsilon_1\ k_{1r} = 1 -$$

With:

$$\{\varepsilon_1 = 1 - \varepsilon_s\ \varepsilon_2 = 1 - \varepsilon_r$$

The parameters of the DFIG obtained after sizing are shown in Table 2.

TABLE II. THE DFIG PARAMETERS OBTAINED

	Symbol	Value
Power	$P_s(kW)$	575.6225
	$P_r(kW)$	115.1245
	$P_{DFIG}(kW)$	
	$r_{is}(mm)$	212.2
	$r_{ir}(mm)$	107.25
	$\xi(mm)$	1.1
Geometric parameters	$r_{os}(mm)$	336.8
	$r_{or}(mm)$	211.1
	$L(mm)$	433.3
	$y_{ds}(mm)$	67.7
	$y_{dr}(mm)$	43.2
	$y_{cs}(mm)$	56.9
	$y_{cr}(mm)$	60.6
	$z_{ds}(mm)$	19
	$z_{dr}(mm)$	18.4
Electrical parameters	$R_s(\Omega)$	0.0115
	$R_r(\Omega)$	0.0876
	$L_s(mH)$	0.304
	$L_r(mH)$	0.185

D. DFIG simulation by FEA

The flux 2D-2022 software has been used to simulate the sized DFIG. For that we make the rotor turn at the nominal speed of 1800 rpm. This corresponds to an operation in supersynchronous mode. We obtain the flux density map and the flux lines of the DFIG which are shown in figures 7 and 8 respectively.

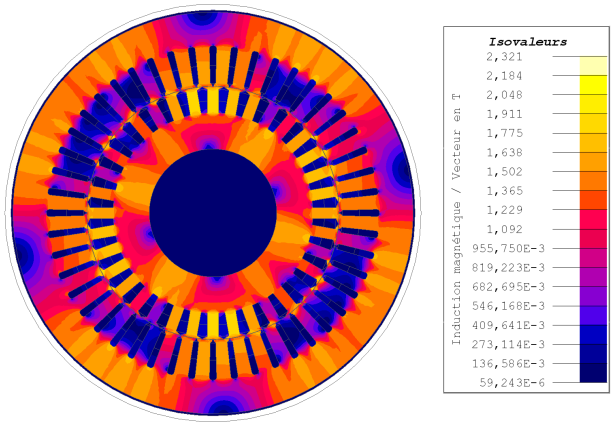

Figure 7. DFIG flux density map

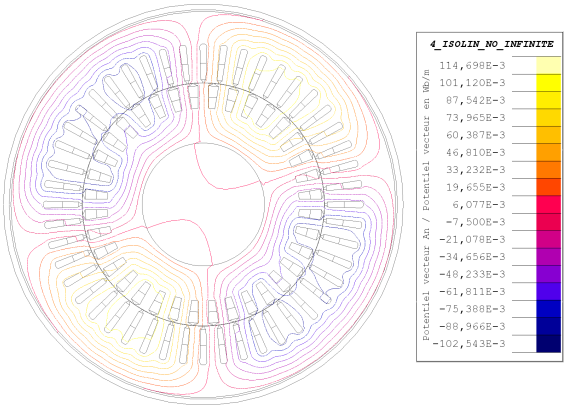

Figure 8. DFIG flux lines map

The figure 9 shows the superposition of the radial and tangential flux densities obtained at the center of the DFIG air gap. It can be noticed that the flux density in the air gap is mainly radial and that it' s not perfectly sinusoidal. This is due to the type of winding used in the rotor.

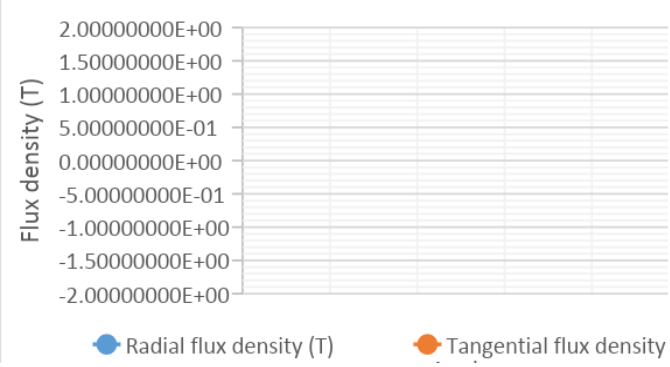

Figure 9. Radial and tangential flux densities curves in the air gap

In the same way the curve of the powers developed by the DFIG in this mode of operation is shown in figure 10.

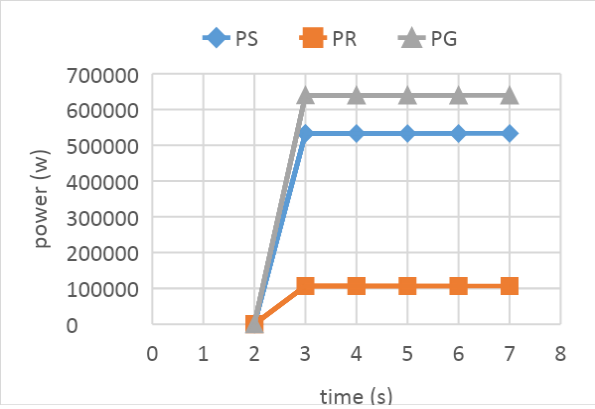

Figure 10. DFIG powers curves

It can be seen that the DFIG takes at most 3s before reaching its steady state. The maximum powers at the stator and rotor are respectively 533.3 kW and 106.66 kW. We then obtain a maximum power of 640 kW developed by the generator.

III. DFIG THERMAL MODEL

To establish the thermal model, it is important to determine the different losses in the generator. These losses are dissipated in the form of heat and are classified into two categories: joule losses and iron losses. The respective stator and rotor losses P_{js} and P_{jr} are calculated analytically by formulas (42) and (43). As for the respective iron losses P_{fs} and P_{fr} at the stator and rotor, they are determined by the FEA.

$$P_{js} = 3R_s I_{sn}^2 \quad (42)$$

$$P_{jr} = 3R_r I_{rn}^2 \quad (43)$$

The values of the different losses are shown in Table 3.

TABLE III. LOSS VALUES AT THE DFIG LEVEL

Losses	Values
$P_{fs}\,(kW)$	1.493
$P_{fr}\,(kW)$	0.391
$P_{js}\,(kW)$	8.868
$P_{jr}\,(kW)$	2.702

We then calculate the heat sources by dividing the losses by the total volumes corresponding to each DFIG domain. Table 4 below summarizes the heat sources obtained.

TABLE IV. HEAT SOURCE IN EACH DOMAIN

Domain	Losses (kW)	Volume (m^3)	Heat source $\left(\frac{W}{m^3}\right)$
Stator winding	8.868	0.013543	6.55×10^5
Rotor winding	2.702	0.008738	3.09×10^5
Stator yoke	1.493	0.079072	1.89×10^4
Rotor yoke	0.391	0.036002	1.09×10^4

Thanks to these data we simulate the DFIG in thermal steady state under 2D flux 2022. The temperature map of the DFIG is shown in figure 11. On this map, we can notice that the temperature of the DFIG varies from 25°C to 92.94°C.

We present on figure 12-a on the one hand a half view of the temperature variations observed at the level of the rotor and stator yokes and on the other hand on figure 12-b a half view of the temperature variations inside the rotor and stator slots.

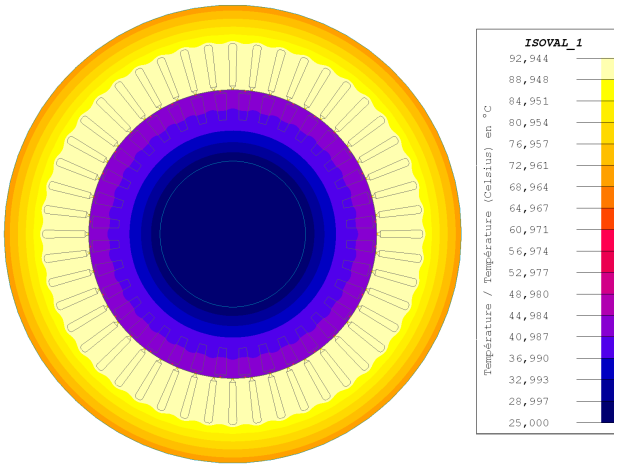

Figure 11. Temperature map of the DFIG

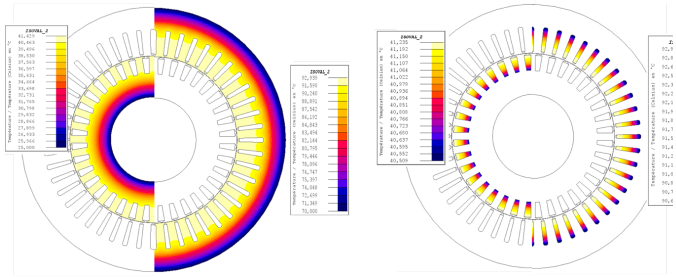

(a) (b)

Figure 12. Half view of the temperature variations. (a) In rotor and stator yokes. (b) Inside the rotor and stator slots

It can be seen that the temperatures in the stator yoke are higher than in the rotor yoke. Similarly, the temperatures in the stator slots are higher than in the rotor slots. This result is normal because the stator windings carry much higher currents than the rotor windings and generate more Joule losses and therefore more heating. The average temperature obtained in the air gap is 67.09 °C.

The minimum and maximum temperature values in each domain of the DFIG are shown in Table 5.

TABLE V. TEMPERATURE VARIATION IN EACH DOMAIN

Domain	Minimum value	Maximum value
Stator winding	$90.6°C$	$92.94°C$
Rotor winding	$40.51°C$	$41.24°C$
Stator yoke	$70°C$	$92.94°C$
Rotor yoke	$25°C$	$41.43°C$
Air gap	$41.3°C$	$92.87°C$

IV. CONCLUSION

In this paper we have sized and simulated a DFIG adapted to the Benin offshore wind profile. For the sizing, we started from an analytical model to obtain the electrical, magnetic and geometrical parameters of the generator. These parameters allowed us to build the dynamic model by FEA in flux-2D_2022. From this model we obtained the powers developed in the stator, in the rotor as well as the total power for an operation in nominal regime. It was found that the obtained powers are close to the calculated theoretical powers. We then developed the thermal model of the DFIG by determining the steady state temperature distribution in the active parts by FEA. The results obtained are satisfactory and can be used for the design of the DFIG. In addition, to complete this work, a study on the optimization and control of the DFIG is underway.

REFERENCES

[1] « Renewable Energy Market Analysis: Africa and its Regions », p. 318.

[2] « The Renewable Energy Transition in Africa », */publications/2021/March/The-Renewable-Energy-Transition-in-Africa*. https://www.irena.org/publications/2021/March/The-Renewable-Energy-Transition-in-Africa (consulté le 1 octobre 2022).

[3] R. Hiremath et T. Moger, « Comparison of LVRT Enhancement for DFIG-Based Wind Turbine Generator with Rotor-Side Control Strategy », in *2020 International Conference on Electrical and Electronics Engineering (ICE3)*, Gorakhpur, India, févr. 2020, p. 216‑220. doi: 10.1109/ICE348803.2020.9122830.

[4] B. Rached, M. Bensaid, M. Elharoussi, et E. Abdelmounim, « DSP in the loop Implementation of the Control of a DFIG Used in Wind Power System », in *2020 1st International Conference on Innovative Research in Applied Science, Engineering and Technology (IRASET)*, Meknes, Morocco, avr. 2020, p. 1‑6. doi: 10.1109/IRASET48871.2020.9092165.

[5] C. E. Prieto Cerón, L. F. Normandia Lourenço, J. S. Solís-Chaves, et A. J. Sguarezi Filho, « A Generalized Predictive Controller for a Wind Turbine Providing Frequency Support for a Microgrid », *Energies*, vol. 15, nº 7, Art. nº 7, janv. 2022, doi: 10.3390/en15072562.

[6] « Ventusky - Cartes de prévision météo ». https://www.ventusky.com (consulté le 1 octobre 2022).

[7] M. R. Gnandji, F.-X. Fifatin, F. Dubas, C. Espanet, et A. Vianou, « Etude du Potentiel Energétique Eolien Offshore du Bénin », Cotonou, Benin, avr. 2018. Consulté le: 1 octobre 2022. [En ligne]. Disponible sur: https://hal.archives-ouvertes.fr/hal-02130123

[8] D.-C. Phan et S. Yamamoto, « Maximum Energy Output of a DFIG Wind Turbine Using an Improved MPPT-Curve Method », *Energies*, vol. 8, nº 10, Art. nº 10, oct. 2015, doi: 10.3390/en81011718.

[9] C. Ulu et G. Kömürgöz, « Electrical design and testing of a 500 kW doubly fed induction generator for wind power applications », *Turk J Elec Eng & Comp Sci*, vol. 25, p. 1278‑1290, 2017, doi: 10.3906/elk-1512-28.

[10] A. Izanlo, S. E. Abdollahi, et S. A. Gholamian, « A New Method for Design and Optimization of DFIG for Wind Power Applications », *Electric Power Components and Systems*, vol. 48, nº 14‑15, p. 1523‑1536, sept. 2020, doi: 10.1080/15325008.2020.1856231.

[11] O. I. Olubamiwa et N. Gule, « Performance investigation of DFIG topologies with different design parameters », in *2017 IEEE AFRICON*, Cape Town, sept. 2017, p. 1242‑1247. doi: 10.1109/AFRCON.2017.8095660.

[12] « I. Boldea, S A. Nasar, "The Induction Machines Design Handbook," Second Edition, 2010. ».

[13] J. Pyrhonen, T. Jokinen, et V. Hrabovcová, *Design of rotating electrical machines*. Chichester, West Sussex, United Kingdom ; Hoboken, NJ: Wiley, 2008.